Performance enhancement of VSAT MC-CDMA system using channel coding techniques and Predistortion over Rayleigh channel

[1]Mohammed EL JOURMI, [2]Hassan EL GHAZI, [1]Abdellatif BENNIS, [3]Hassan OUAHMANE
[1]Physics Department, Hassan II University, FSBM, Casablanca, Morocco
[2]Telecommunications Department, INPT, Rabat, Morocco
[3]Networks and Telecommunications Department, ENSA, El jadida, Morocco

Abstract: - In this paper, the performance of VSAT network, in uplink (earth station to a geostationary satellite) and Ku-band have been examined over Rayleigh channel. The most popular type of multiple access schemes: Code Division Multiple Access (CDMA) combined with the multi-carrier transmission system OFDM is used in this study, in order to obtain a densification of data traffic on the network and achieve a high data rate. To improve the performance of the envisaged system, and get a very low bit error rate, we proposed the use of strategies allowing the correction of errors induced by the imperfections of the communication channel. Channel coding techniques used in this study are (LDPC codes, Turbo codes and convolutional codes). In the simulation results, we have demonstrated the effectiveness of each coding strategy in our communication system. The integration of LDPC coding in our transmission chain has provided a significant gain compared to other encoding schemes, and the bit error rate (BER) has reached a satisfying level at a low energy per bit to noise power spectral density ratio (E_b/N_0). To compensate the effect of the non-linearity of the High Power Amplifier HPA, a predistortion technique is adopted to further improve performance of the envisaged system.

Key-Words: - VSAT Network, MC-CDMA scheme, Channel coding, predistortion, Ku band, Uplink.

1 Introduction

Today's satellites can be used in many communication services requiring point to point or point to multipoint. The use of satellites has solved some problems in communication domain and this basically amounts to the large area of coverage provided by them. Thus, communication between remote ground stations geographically is become possible with the first commercial communications satellite "Early Bird". The field of satellite communications is still on a path of improvement, but the major problem hindering its progress is the presence of random errors on the satellite link and that can significantly degrades the system performance. For this reason we used channel coding mechanisms to reduce the error rate and improve the system performance.

The objective of this paper is to design a satellite ground segment component for use in telecommunications and analyze its performance. Therefore, the ground segment is designed to fit in the description of a Very Small Aperture Terminal (VSAT), which requires antenna dimensions less than 1.8 m in diameter. The designed system has a wide bandwidth and use MC-CDMA scheme. In this study, the BPSK is preferred for their low latency in the modulation or demodulation process. In the event of the destruction of the orthogonality between user codes, the resulting multiple access interference (MAI) severely limits the system performance. In order to reduce the bit error rate caused by intersymbol interference (ISI) or multiple access interference (MAI) channel coding (LDPC codes, Turbo codes and Convolutional codes) is applied which can make error detection and correction at the receiver. An adaptive equalization technique must be used to compensate distortions caused by propagation environment. Therefore, the use of MMSE technique is able to improve performance of the envisaged system in multipath-interference environments. To be able to send signals through great distance, the signals need to be amplified before transmission. The High Power Amplifier (HPA) of Rapp's model which is based on a Solide State Power Amplifier (SSPA) is used and a low noise amplifier (LNA) is used to amplify very weak signals captured by an antenna. To compensate the effect of the non-linearity in the communication system, a predistortion process adapted to the SSPA amplifier is proposed. In this study, the CDMA encoder uses PN sequences and Walsh Codes to generate a spread signal. Each VSAT uses a different PN sequence and each user in a VSAT uses different Walsh Codes.

This paper is organized as follows. In Section 2 the VSAT Network are briefly described with its configurations. The principle of MC-CDMA scheme is presented with modeling of proposed system in Section 3. Section 4 presents the convolutional codes principle. Sections 5 and 6, respectively,

describe the principle of Turbo coding and LDPC codes. In section 7 the simulation model and system specifications are presented. Simulation results are presented in Section 8, and conclusions are drawn in Section 9.

2 VSAT Network

The satellite communications networks using Very Small Aperture Terminals (VSAT) appeared in the 1980s. The appearance of these terminals amounts in particular to the companies which wish to rent analog or digital telephone lines with low cost. VSATs networks allow bidirectional satellite communication (i.e. earth stations play the role of a transmitter and receiver), which eliminates terrestrial link, unless the user wishes to communication relief and to provide another type of application such as video on demand [3].

There are two major network configurations viz: the hub-based star VSAT network, which provides a "star" type of topology, and the "mesh" network, which allows connections between any pair of VSATs.

2.1 Meshed configuration

As all the VSATs are visible from the satellite, carriers can be relayed by the satellite from any VSAT to any other VSAT in the network as shown in figure 1. This type of configuration is called point-to-point topology. In this mesh type, earth stations communicate directly via satellite and will have only one hop communication.

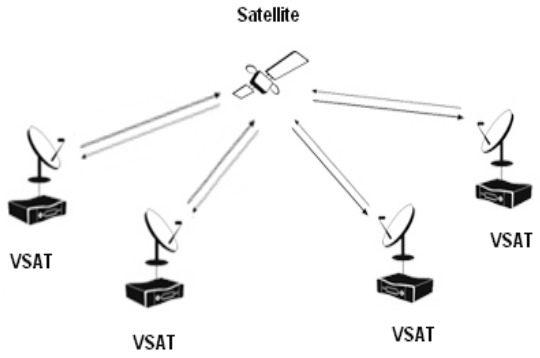

Fig. 1 Meshed topology of VSAT Network

2.2 Star configuration

This configuration is based on a station larger than a VSAT in the network, called the hub. The hub station has a larger antenna size than that of a VSAT, about 4m to 11m resulting in a higher gain than that of a typical VSAT antenna, and is equipped with a more powerful transmitter [5]. As a result of its improved capability, the hub station is able to receive adequately all carriers transmitted by the VSATs, and to convey the desired information to all VSATs by means of its own transmitted carriers. The architecture of the network becomes star as shown in figure 2. The links from the hub to the VSAT are named "outbound links" and the ones from the VSAT to the hub are named "inbound links". Both inbound and outbound links consist of two links, uplink and downlink, to and from the satellite.

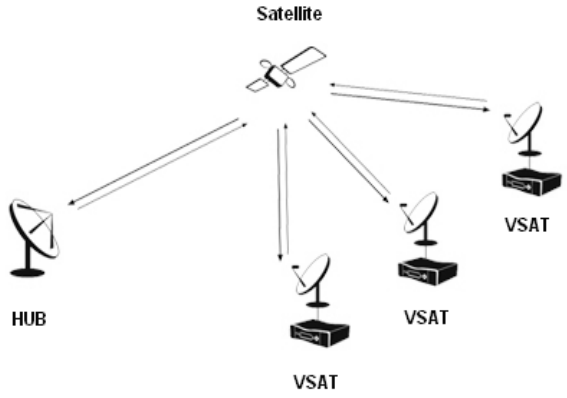

Fig. 2 Star topology of VSAT Network

In conclusion, star configuration is imposed by power requirements resulting from the reduced size and hence the low cost of the VSAT earth station in conjunction with power limitation of the satellite. Meshed configuration is considered whenever such limitations do not hold, or are unacceptable. Meshed networks have the advantage of a reduced propagation delay (single hop delay is 0.25 sec instead of 0.5 sec for double hop) which is especially of interest for telephone service [2].

3 Multi-carrier CDMA

Multi-carrier CDMA system is based on a combination of the CDMA scheme and orthogonal frequency division multiplexing (OFDM) signaling.

MC-CDMA transmitter spreads the original signal using a given spreading code in the frequency domain. In other words, a fraction of the symbol corresponding to a chip of the spreading code is transmitted through a different subcarrier.

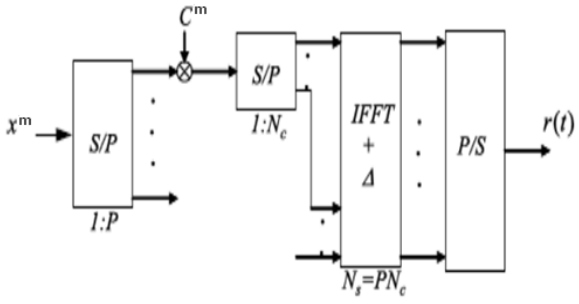

Fig. 3 MC-CDMA Transmitter

The figure 3 shows the MC-CDMA transmitter for the mth user. The input information sequence is first converted into P parallel data sequences, and then each Serial/Parallel converter output is multiplied with the spreading code with length L_C. All the data in total $N = P \times L_C$ (corresponding to the total number of subcarriers) are modulated in baseband by the inverse Fast Fourier transform (IFFT) and converted back into serial data. The guard interval Δ is inserted between symbols to avoid intersymbol interference, and finally the signal is transmitted.

Figure 4 shows the MC-CDMA receiver. It requires coherent detection for successful despreading operation and this causes the structure of MC-CDMA receiver to be very complicated. In figure, the k-subcarrier components (k=1,2,…Lc) corresponding to the received data y^m is first coherently detected with FFT and then multiplied with the gain G to combine the energy of the received signal scattered in the frequency domain [6]-[7].

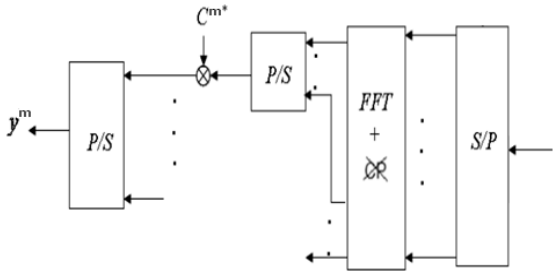

Fig. 4 MC-CDMA Receiver

3.1 Transmitter model of envisaged system

Transmitted signal S(t) corresponding to the lth data bit of the mth user is defined by:

$$S(t) = \sqrt{\frac{2P_{\alpha,m}}{N}} \sum_{v=0}^{S-1} \sum_{l=-\infty}^{+\infty} \sum_{n=0}^{N-1} W_{\alpha,m}[n]\, b_{\alpha,m}[l] \cos\left(2\pi\left(f_c + \frac{n}{T_b}\right)t\right) C_\alpha[v]\, U_{T_b}(t - lT_b) \quad (1)$$

Where $P_{\alpha,m}$ is the power of data bit, $U_{T_b}(t - lT_b)$ is the rectangular pulse defined in the $[0, T_b]$. Every user has a spreading code $W_{\alpha,m}[n]$ with $n = 0,1,\dots,N-1$ and N is the length of the sequence chip. The same signature sequence chip is used to modulate each of the N carriers of the mth user. The maximum number of users in the system is M. Every VSAT has a signature $C_\alpha[v]$ with $v = 0,1,\dots,S-1$ and S is the length of the spreading code. α denote the number of VSATs with $\alpha = 1,2,\dots,K$ and K is the maximum number of VSATs.

3.2 Receiver model of system over Rayleigh channel

The receiver signal of M active users in the VSAT-MC-CDMA system can be written as:

$$R(t) = \sum_{\alpha=1}^{K} \sum_{v=0}^{S-1} \sum_{m=0}^{M-1} \sum_{l=-\infty}^{+\infty} \sum_{n=0}^{N-1} \sqrt{\frac{2P_{\alpha,m}}{N}}\, \varphi_{\alpha,m,n} W_{\alpha,m}[n] b_{\alpha,m}[l] \cos\left(2\pi\left(f_c + \frac{n}{T_b}\right)t + \psi_{\alpha,m,n}\right) C_\alpha[v]\, U_{T_b}(t - lT_b) + n(t) + \xi(t) \quad (2)$$

Where $\varphi_{\alpha,m,n}$ and $\psi_{\alpha,m,n}$ are respectively fading amplitude and phase shift. n(t) is the additive white Gaussian noise (AWGN) with double sided power spectral density of $N_0/2$ and $\xi(t)$ is the inter-VSAT interference.

3.3 The Decision Statistic

The information bits $b_{\beta,j,n}$ received from a user specified (m = j) and VSAT ($\alpha = \beta$) will be used for this analysis. ($\alpha = \beta$) and (m = j) are the indices of despreaded information bits we want to retrieve. All other values of α ($\alpha \neq \beta$) and m ($m \neq j$) will be considered co-channel interference and inter-VSATs interference.

Assuming that users are synchronous in time, after demodulation and combination of sub-carrier signals, the decision variable is obtained as:

$$\mathcal{Y}_{\beta,j,l} = \frac{1}{T_b} \int_{lT_b}^{(l+1)T_b} R(t) \sum_{n=0}^{N-1} G_{\beta,j,n} W_{\beta,j}[n] \cos\left(2\pi\left(f_c + \frac{n}{T_b}\right)t + \hat{\psi}_{\alpha,m,n}\right) C_\beta[v]\, dt \quad (3)$$

Where $G_{\beta,j,n}$ is the equalizing coefficient of the user j from the earth station β.

The decision variable consists of four components, the first term corresponds to the desired signal, the second term corresponds to the multiple access interference from other users, the third term corresponds to the noise and the last term represents the interference between VSATs.

$$\mathcal{Y}_{\beta,j,l} = \mathcal{D} + \mathcal{MAI} + \eta + \zeta \quad (4)$$

$\mathcal{D}$: Signal désiré

$\mathcal{MAI}$: Interférence Co-canal

η : Bruit blanc gaussien additif

ζ : Interférence entre VSATs

Note that the absence of interference between symbols and the interference between carriers is ensured by the use of a guard interval longer than the delay spread of the channel impulse response.

Components of the decision variable can be written in the following form:

- Desired signal

$$\mathcal{D} = \frac{1}{2}\sqrt{\frac{2\mathrm{P}_{\beta,\mathrm{j}}}{\mathrm{N}}}\sum_{\mathrm{l}=-\infty}^{+\infty}\sum_{\mathrm{n}=0}^{\mathrm{N}-1}(S-1)\varphi_{\beta,\mathrm{j,n}}\ \mathrm{b}_{\beta,\mathrm{j}}[\mathrm{l}]\mathrm{G}_{\beta,\mathrm{j,n}} \tag{5}$$

- Co-channel interference

$$\mathcal{MAI} = \sum_{\substack{m=0\\ m\neq j}}^{M-1}\sum_{\mathrm{l}=-\infty}^{+\infty}\sum_{\mathrm{n}=0}^{\mathrm{N}-1}\frac{1}{2}\sqrt{\frac{2\mathrm{P}_{\beta,\mathrm{m}}}{\mathrm{N}}}\varphi_{\beta,\mathrm{m,n}}\ \mathrm{b}_{\beta,\mathrm{m}}[\mathrm{l}]\mathrm{G}_{\beta,\mathrm{j,n}}\mathrm{W}_{\beta,\mathrm{m}}[\mathrm{n}]\mathrm{W}_{\beta,\mathrm{j}}[\mathrm{n}]\cos(\psi_{\beta,\mathrm{j,n}}-\psi_{\beta,\mathrm{m,n}}) \tag{6}$$

- Noise

$$\eta = \sum_{v=0}^{\mathrm{S}-1}\sum_{\mathrm{n}=0}^{\mathrm{N}-1}\frac{1}{\mathrm{T_b}}\int_{\mathrm{lT_b}}^{(\mathrm{l}+1)\mathrm{T_b}}\mathrm{n(t)}\mathrm{G}_{\beta,\mathrm{j,n}}\mathrm{W}_{\beta,\mathrm{j}}[\mathrm{n}]\mathrm{C}_{\beta}[v]\cos\left(2\pi\left(\mathrm{f_c}+\frac{\mathrm{n}}{\mathrm{T_b}}\right)\mathrm{t}+\psi_{\beta,\mathrm{j,n}}\right)\mathrm{dt} \tag{7}$$

- Inter-VSATs interference

$$\zeta = \sum_{\substack{\alpha=1\\ \alpha\neq\beta}}^{\mathrm{K}}\sum_{v=0}^{\mathrm{S}-1}\sum_{\mathrm{m}=0}^{\mathrm{M}-1}\sum_{\mathrm{l}=-\infty}^{+\infty}\sum_{\mathrm{n}=0}^{\mathrm{N}-1}\frac{1}{2}\sqrt{\frac{2\mathrm{P}_{\alpha,\mathrm{m}}}{\mathrm{N}}}\ \varphi_{\alpha,\mathrm{m,n}}\mathrm{W}_{\alpha,\mathrm{m}}[\mathrm{n}]\mathrm{b}_{\alpha,\mathrm{m}}[\mathrm{l}]\mathrm{G}_{\beta,\mathrm{j,n}}\mathrm{C}_{\alpha}[v]\mathrm{W}_{\beta,\mathrm{j}}[\mathrm{n}]\mathrm{C}_{\beta}[v]\cos\left(\psi_{\beta,\mathrm{j,n}}-\psi_{\alpha,\mathrm{m,n}}\right) \tag{8}$$

Generally speaking the jth user from the βth earth station, the SNIR can be expressed as:

$$SNIR = \frac{E\left[\left(\mathcal{Y}_{\beta,j}\middle|\varphi_{\beta,\mathrm{j}}\right)^2\right]}{\sigma\left(\mathcal{Y}_{\beta,j}\middle|\varphi_{\beta,\mathrm{j}}\right)} \tag{9}$$

Where $\vec{\varphi}_{\beta,\mathrm{j}} = [\vec{\varphi}_{\beta,\mathrm{j},0}, \vec{\varphi}_{\beta,\mathrm{j},1}, \ldots, \vec{\varphi}_{\beta,\mathrm{j},\mathrm{N}-1}]$ is the vector of fading amplitudes of the user j from the earth station β. σ is variance.

Assume independent users and independent subcarriers,

$$E\left[\left(\mathcal{Y}_{\beta,j}\middle|\varphi_{\beta,\mathrm{j}}\right)^2\right] = \frac{1}{4}\frac{2P_{\beta,j}}{N}(S-1)^2\left(\sum_{n=0}^{N-1}\varphi_{\beta,\mathrm{j,n}}\mathrm{G}_{\beta,\mathrm{j,n}}\right)^2 \tag{10}$$

$$\sigma\left(\mathcal{Y}_{\beta,j}\right) = \sigma(\eta)+\sigma(\mathcal{MAI})+\sigma(\zeta) \tag{11}$$

$$\sigma\left(\mathcal{Y}_{\beta,j}\right) = E\left[(\eta)^2\right]+E\left[(\mathcal{MAI})^2\right]+E\left[(\zeta)^2\right] \tag{12}$$

The variance of the noise components is:

$$\sigma\left(\eta\middle|\varphi_{\beta,\mathrm{j}}\right) = \frac{N_0}{4T}\sum_{n=0}^{N-1}G^2{}_{\beta,j,n} \tag{13}$$

The variance of the MAI can be expressed as

$$\sigma\left(\mathcal{MAI}\middle|\varphi_{\beta,\mathrm{j}}\right) = \frac{1}{8}\sum_{\substack{m=0\\ m\neq j}}^{M-1}\sum_{n=0}^{N-1}\frac{2P_{\beta,m}}{N}E\left[\varphi_{\beta,m,n}\right]G^2{}_{\beta,j,n} \tag{14}$$

The variance of the inter-VSAT interference is:

$$\sigma\left(\zeta\middle|\varphi_{\beta,\mathrm{j}}\right) = \frac{1}{8}\sum_{\substack{\alpha=1\\ \alpha\neq\beta}}^{K}\sum_{m=0}^{M-1}\sum_{n=0}^{N-1}\frac{2P_{\alpha,m}}{N}(S-1)^2 E\left[\varphi_{\alpha,m,n}\right]G^2{}_{\beta,j,n} \tag{15}$$

The following expression is the total variance of noise plus interferences of proposed system:

$$\sigma\left(\mathcal{Y}_{\beta,j}\middle|\varphi_{\beta,\mathrm{j}}\right) = \frac{N_0}{4T}\sum_{n=0}^{N-1}G^2{}_{\beta,j,n} + \frac{1}{8}\sum_{\substack{m=0\\ m\neq j}}^{M-1}\sum_{n=0}^{N-1}\frac{2P_{\beta,m}}{N}E\left[\varphi_{\beta,m,n}\right]G^2{}_{\beta,j,n} + \frac{1}{8}\sum_{\substack{\alpha=1\\ \alpha\neq\beta}}^{K}\sum_{m=0}^{M-1}\sum_{n=0}^{N-1}\frac{2P_{\alpha,m}}{N}(S-1)^2 E\left[\varphi_{\alpha,m,n}\right]G^2{}_{\beta,j,n} \tag{16}$$

4 Convolutional codes

A convolutional encoder generates code symbols for transmission utilizing a sequential finite-state machine driven by the information sequence. Decoding these codes then amounts to sequentially observing a corrupted version of the output of this system and attempting to infer the input sequence. From a formal perspective, there is no need to divide the message into segments of some specific length.

Figure 5 illustrates one of the simplest nontrivial convolutional encoders. It is implemented by a shift register of memory (number of delay elements) m = 2 and three summers $\oplus$ over Galois field GF(2). The rate of the code is r = 1/2. The information

sequence . . . $\beta_0, \beta_1, \ldots, \beta_n \ldots, \beta_n \in \{0, 1\}$, is the input sequence of the encoder. The encoder is a finite-state machine that can be described in terms of its state transition diagram. This is shown in Figure 6, where the nodes refer to the contents of the register just before the next input bit arrives. The encoder inputs . . . $\beta_0, \beta_1, \ldots, \beta_n, \ldots$, and outputs . . . $\alpha_0, \alpha_1, \ldots, \alpha_n, \ldots, \beta_n, \alpha_n \in \{0, 1\}$ (2 output symbols per input bit for the rate r = 1/2 encoder) are shown as labels on the transition branches[9]

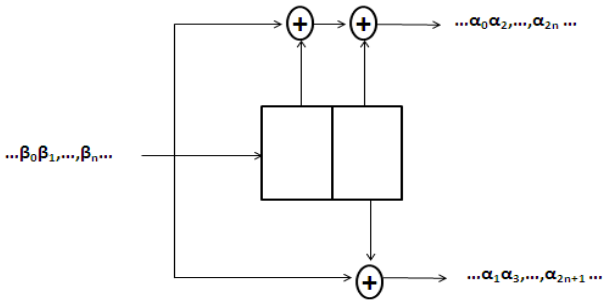

Fig. 5 A rate r = 1/2 memory m = 2 convolutional encoder

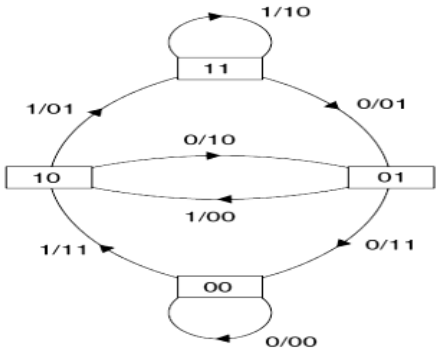

Fig. 6 The state-transition diagram for the encoder in Figure 5

Decoding of convolutional codes is a more difficult problem than encoding. The function of a convolutional decoder is estimating the encoded input information using a method that results in the minimum possible number of errors. Unlike a block code, a convolutional code is a finite state machine. Therefore, the output decoder is a "maximum likelihood estimator" and optimum decoding is done by searching through the trellis for the most probable sequence. Depending on whether hard decision or soft decision decoding is used, either the Hamming or Euclidian metric is used, respectively.

Convolutional coding can be decoded with several different algorithms. The Viterbi algorithm is the most commonly used, and for this reason we adopted the Viterbi decoder to decode the data encoded with Convolutional encoder.

5 Turbo codes

Parallel-concatenated convolutional codes (PCCCs), also known as turbo codes, were first introduced by Berrou, Galvieux and Thitimajshima in 1993 [11] and have been shown to offer near-capacity performance for large block sizes. This turbo code is constructed by parallel concatenation of two or more convolutional constituent codes with an interleaver. Encoder and decoder for rate 1/3 turbo code are illustrated in Fig.7 and Fig.8.

One of the key advantages of turbo codes is that they can be decoded by a practical decoding scheme for which the decoding complexity only grows linearly in the length of the code. In general, the complexity of maximum-likelihood (ML) decoding grows exponentially in the length of the code.

5.1 Turbo encoder

In Figure 7 the turbo encoder consists of two convolutional encoders and an interleaver and it produces a recursive Parallel Concatenated Convolutional Code (PCCC). Here the first constituent encoder receives input bits directly, whereas the second constituent encoder is fed with input bits through the interleaver. Furthermore the figure shows that the entire turbo encoder is an 1/3 rate encoder, thus for each input, three outputs are generated. This rate is however altered depending on possible puncturing of bits and tail bits from the second constituent encoder at termination [10].

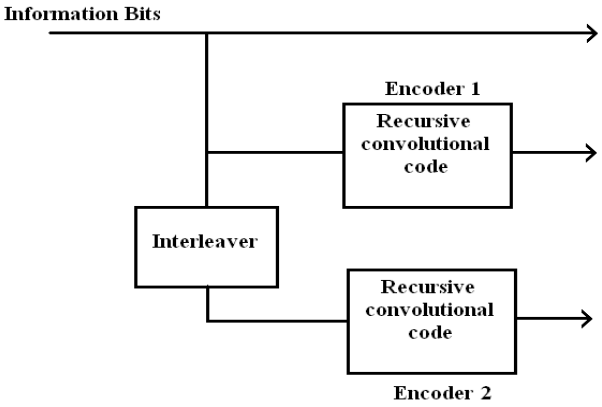

Fig. 7 A rate 1/3 Turbo code encoder

5.2 Turbo decoder

The job of the turbo decoder is to reestablish the transmitted data from the received systematic bitstream and the two parity check bitstreams, even though these are corrupted by noise.

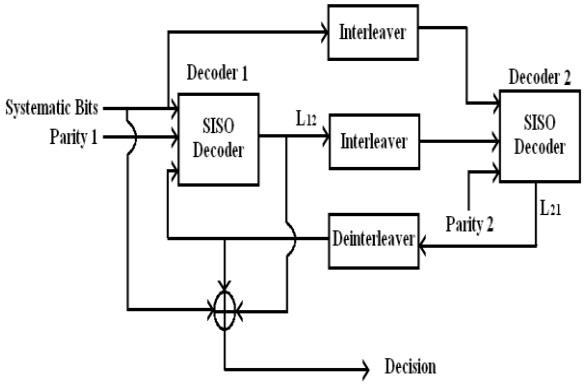

Fig. 8 A rate 1/3 Turbo code decoder

In a typical turbo decoding system (see Fig.8), two decoders operate iteratively and pass their decisions to each other after each iteration. These decoders should produce soft-outputs to improve the decoding performance. Such a decoder is called a Soft-Input Soft- Output (SISO) decoder [10]. Each decoder operates not only on its own input but also on the other decoder's incompletely decoded output.

In this paper the two SISO decoders used for turbo decoding are Max-Log-Map.

6 LDPC codes

LDPC codes were invented by Robert Gallager [11] in his PhD thesis. Soon after their invention, they were largely forgotten, and reinvented several times for the next 30 years. Their comeback is one of the most intriguing aspects of their history, since two different communities reinvented codes similar to Gallager's LDPC codes at roughly the same time, but for entirely different reasons.

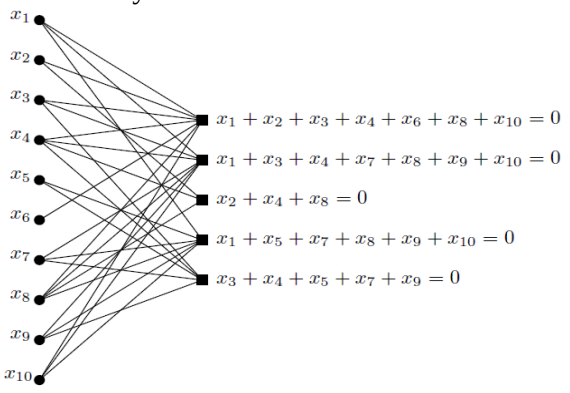

Fig. 9 An LDPC code

LDPC codes are linear codes obtained from sparse bipartite graphs. Suppose that G is a graph with n left nodes (called message nodes) and r right nodes (called check nodes). The graph gives rise to a linear code of block length n and dimension at least $n - r$ in the following way: The n coordinates of the codewords are associated with the n message nodes. The codewords are those vectors $(c_1, \ldots, c_n)$ such that for all check nodes the sum of the neighboring positions among the message nodes is zero. Figure 9 gives an example.

The graph representation is analogous to a matrix representation by looking at the adjacency matrix of the graph: let H be a binary $r \times n$-matrix in which the entry (I, j) is 1 if and only if the ith check node is connected to the jth message node in the graph. Then the LDPC code defined by the graph is the set of vectors $c = (c_1, \ldots, c_n)$ such that $H.c^T = 0$. The matrix H is called a parity check matrix for the code. Conversely, any binary $r \times n$-matrix gives rise to a bipartite graph between n message and r check nodes, and the code defined as the null space of H is precisely the code associated to this graph. Therefore, any linear code has a representation as a code associated to a bipartite graph (note that this graph is not uniquely defined by the code). However, not every binary linear code has a representation by a sparse bipartite graph. If it does, then the code is called a low-density parity-check (LDPC) code.

The sparsity of the graph structure is key property that allows for the algorithmic efficiency of LDPC codes.

6.1 Decoding Algorithms: Belief Propagation

Let us first start by describing a general class of decoding algorithms for LDPC codes. These algorithms are called message passing algorithms, and are iterative algorithms. The reason for their name is that at each round of the algorithms messages are passed from message nodes to check nodes, and from check nodes back to message nodes. The messages from message nodes to check nodes are computed based on the observed value of the message node and some of the messages passed from the neighboring check nodes to that message node. An important aspect is that the message that is sent from a message node v to a check node c must not take into account the message sent in the previous round from c to v. The same is true for messages passed from check nodes to message nodes.

One important subclass of message passing algorithms is the belief propagation algorithm. This algorithm is presented in Gallager's work, and it is also used in the Artificial Intelligence community. The messages passed along the edges in this algorithm are probabilities, or beliefs. More precisely, the message passed from a message node v to a check node c is the probability that v has a

certain value given the observed value of that message node, and all the values communicated to v in the prior round from check nodes incident to v other thanc. On the other hand, the message passed from c to v is the probability that v has a certain value given all the messages passed to c in the previous round from message nodes other thanv.

7 Simulation model and system specifications

This section is devoted to the description of the simulation model, and presents the main characteristics and specifications of the proposed system.

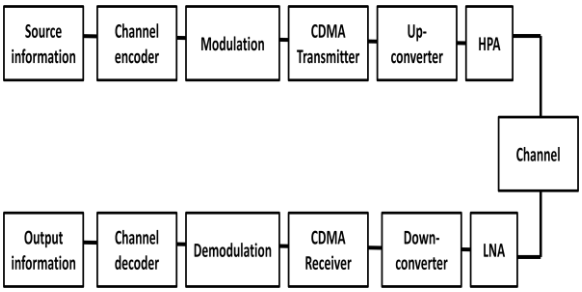

Fig. 10 Overall Simulation Block Diagram

Figure 10 illustrates the overall simulation model. Binary input signal to the system is converted to symbol stream after passing through the encoder. The frequency domain spreading is done by using signature sequence of length 32 in the CDMA transmitter. Up-converter is capable of outputting its carrier at the desired RF frequency. Signal is amplified with HPA before being transmitted through the transmission channel. LNA amplify very weak signals captured by the VSAT antenna. Down-converter converts the desired signal band to a convenient IF frequency for digitization. Despreading in the CDMA receiver, demodulation is done before passing through the decoder. The original binary data is recovered after passing through the decoder [8]. The parameters that we use in our simulation are as follows:

TABLE 1: GENERAL INFORMATION

Satellite orbit radius	42242 km
Earth radius	6370 km
Distance from the VSAT to satellite	38054 km
Free space loss	206.1 dB
Speed of light, c	3.108 ms-1
Boltzmann's constant	-228.6 dBJK-1 (=1.38 × 10−23J/K)

TABLE 2: VSAT PARAMETERS

up-link frequency F_u	14.25 GHz
VSAT HPA output power P_{TxVSAT}	1 W
Antenna diameter	1.2 m
Antenna gain	42.84 dBi
EIRP	42.84 dBW
VSAT latitude	45.5° N
VSAT longitude	9.5° E
Elevation angle	37.56°
Azimuth angle	183.5°

TABLE 3: SATELLITE PARAMETERS

Satellite figure of merit $(G/T)_{SL}$	-1 dB/K
satellite receiver effective input noise temperature	500 K
Satellite antenna noise temperature	290 K
uplink system noise temperature	790 K
Power Flux density ϕ	-119.22 dBW/m^2
Transponder bandwidth	54 MHz
Satellite antenna gain	31 dBi
Sub-satellite point longitude	7° E
C/N_0 in up-link	64.34 dBHz

8 Results and discussion

In this simulation the performance results of VSAT MC-CDMA system are obtained for uncoded system and coded system with different channel coding schemes and by using Binary Phase Shift Keying modulation over Rayleigh channel. In this

simulation the number of sub-carriers equals the number of chips of the spreading code, the maximum number of users is 32 users (full loading) and the code length of spreading code is 32 chips.

8.1 Performance of uncoded VSAT MC-CDMA system

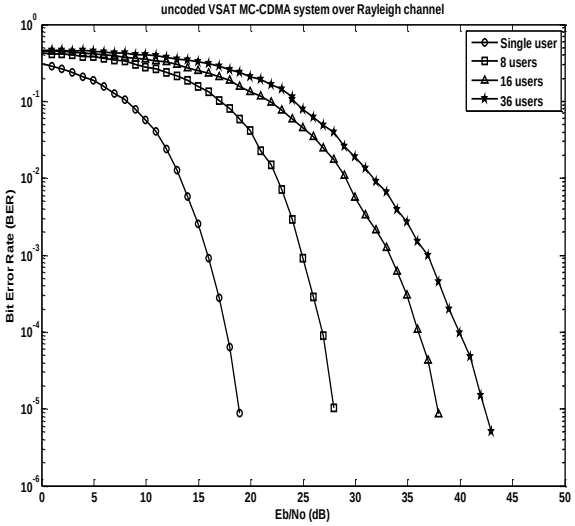

Fig.11 Performance of uncoded VSAT MC-CDMA system (for single, 8, 16 and 32 users)

Figure 11 shows the performance of VSAT MC-CDMA system over Rayleigh channel for single, 8, 16 and 32 users. As seen in the figure, we can see that the difference of performance curves is due to the difference in number of active users in the network. It is observed that the performance obtained in the single-user case was better in comparison with those of 8, 16 and 32 users. We can also note that the performance is not very good without coding, and it degrades rapidly as the total number of users increase.

For different number of users the BER performance achieves up to 10^{-6}. For single user the E_b/N_0 is beyond 19 dB and for half loading (16 users) the E_b/N_0 is beyond 38 dB. For full loading (32 users) the E_b/N_0 is beyond 43 dB.

8.2 Performance of VSAT MC-CDMA system using convolutional code

The simulation results of the system using convolutional coding over Rayleigh channel are shown in Figure 12. The decoder type used for convolutional coding is the Viterbi decoder with code rate $R = \frac{1}{3}$.

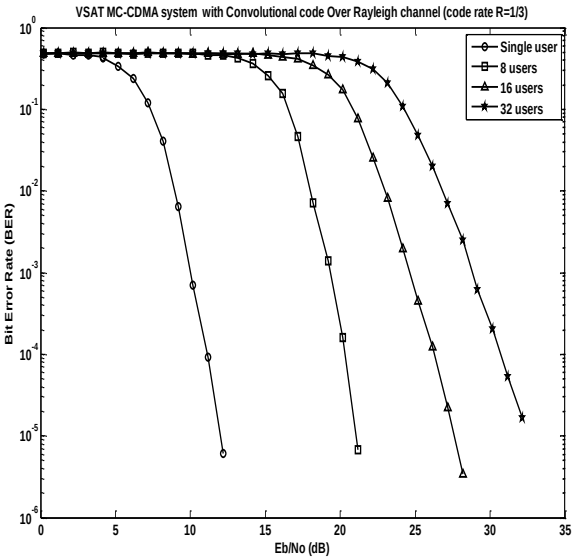

Fig.12 Performance of VSAT MC-CDMA system using Convolutional code (for single, 8, 16 and 32 users)

We analyse the results of the Figure 12, we note that the use of convolutional coding significantly improves the performance of VSAT MC-CDMA. Indeed, for 32 users active in the network, we notice that there is an additional gain of 9 dB offered for a bit error rate 2.10^{-5}.

8.3 Performance of VSAT MC-CDMA system using Turbo codes

To evaluate the performance of the system using turbo coding in a multipath environment, we used the SISO decoder, which is carried out by using the Max-Log-Map algorithm. In this simulation we stopped at 3th iteration since there is no additional improvement in term of BER for further iterations.

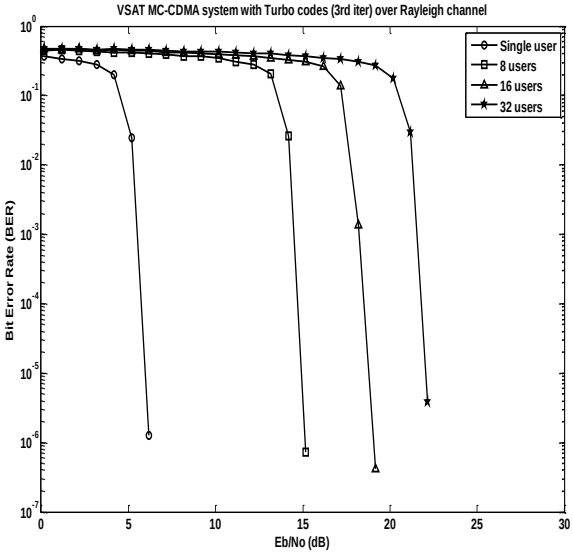

Fig.13 Performance of VSAT MC-CDMA system using Turbo codes (For Single, 8, 16 and 32 users)

On figure 13 we show the results of the third iteration obtained by the simulation of VSAT MC-CDMA system, for a variation of the active users number in the network. As can be observed, for a full loading of the network and for a bit error rate of 10^{-5}, the iterative process provides a gain of approximately 6 dB compared with the performance of the system using convolutional coding (for a similar number of users).

We can conclude that the performance of VSAT MC-CDMA system has been improved when the iterative turbo coding is used. The latter has provided advantageous performance compared to convolutional coding system, but in terms of complexity, the iterative turbo decoding is more complex compared to Viterbi decoding.

8.4 Performance of VSAT MC-CDMA system using LDPC codes

The decoder algorithm used for LDPC is the Belief Propagation with $R = \frac{1}{3}$. For different number of active users in the network, the performance results of the envisaged system, using LDPC codes are showed in the figure 14.

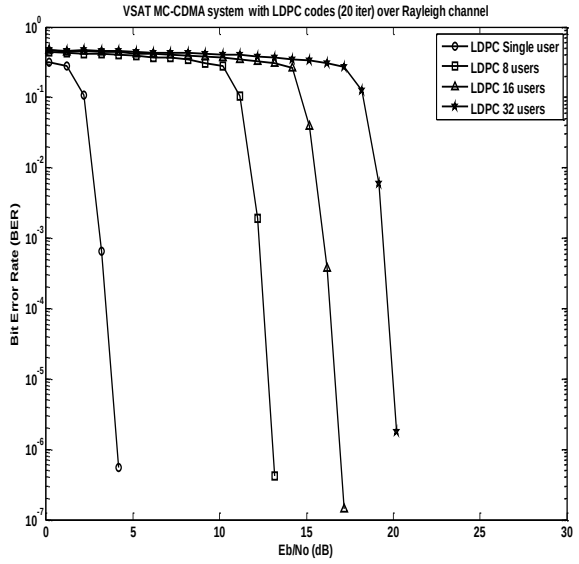

Fig.14 Performance of VSAT MC-CDMA system using LDPC codes (For Single, 8, 16 and 32 users)

In our simulation we stopped at 20th iteration since there is no additional improvement in term of BER for further iterations. In comparison with previously reported results, we note that system using LDPC coding showed better performance compared to the system adopting the Turbo coding. In the figure it is observed that for a bit error rate of the system opting to the LDPC coding provides an additional gain of 2 dB (for 32 users) compared with coded system by Turbo code (for similar number of users). In terms of BER, the performance of system using LDPC reaches a lower value compared with that achieved by the use of Turbo coding. In terms of complexity, we find that the LDPC decoding system is less complex compared to Turbo decoding process.

8.5 Performance of VSAT MC-CDMA system using the predistortion technique

This part is devoted to the description of the linearization technique principle adapted to the power amplifier adopted by VSATs stations, and analysis of simulation results obtained by the VSAT MC-CDMA system using LDPC codes in conjunction with the predistortion process.

8.5.1 Predistortion technique

SSPA and TWTA are two types of power amplifiers which are widely used by the VSAT networks. TWTA is mostly used for high power satellite transmitters (in this case, we talk about the HUB stations), while SSPA is used in many other applications requiring stations with small antenna (as the case of VSATs stations).

To compensate the effect of non-linearity of the High Power Amplifier (HPA), we introduced in the communication system a predistortion technique which is adapted to the SSPA amplifier.

The complex output of RF with non-linear distortion can be expressed as:

$$z(t) = A\left[\rho(t)\right].\exp\left[\, j\left(\varphi(t) + \Phi\left[\rho(t)\right]\right)\right] \quad (17)$$

Where A (ρ) and φ(ρ) represent the conversion AM/AM and AM/PM of the nonlinear amplifier.

The SSPA's AM/AM and AM/PM can be captured by [12][13]:

$$A\left[\rho(t)\right] = \frac{\rho(t)}{\left[1 + (\rho(t)/A_0)^{2p}\right]^{1/2p}} \quad (18)$$

$$\Phi\left[\rho(t)\right] \cong 0 \quad (19)$$

A_0 is the maximum output amplitude and the parameter p controls the smoothness of the transition from the linear region to the limiting region [13].

In general, the predistortion technique principle is illustrated in the Figure 15.

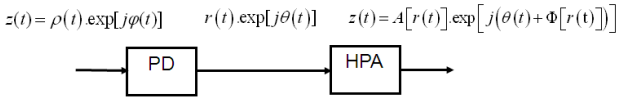

Fig.15 predistortion technique principle

When a PD transformation is applied to the signal, this last will pass through the HPA in order to be amplified and the nonlinearity effects of the amplifier will be compensated. For the predistortion technique, the input-output relationship is given by the following expressions:

$$r(t)=A^{-1}[\rho(t)] \tag{20}$$

$$\theta(t)=\varphi(t)-\Phi[r(t)] \tag{21}$$

The linearization technique chosen in our study is the predistortion described in [14]. Therefore by inversion of A (ρ) we get the expression of $r(t)$ corresponding to the SSPA amplifier.

$$r(t)=\frac{\rho(t)}{[1-(\rho(t)/A_0)^{2p}]^{1/2p}} \tag{22}$$

8.5.2 Simulation results of VSAT MC-CDMA with predistortion technique

To highlight the improvement provided by the predistortion technique in the VSAT MC-CDMA system using the LDPC coding, we have shown in Figure 16 the performance curves of the system with and without integrating the predistortion.

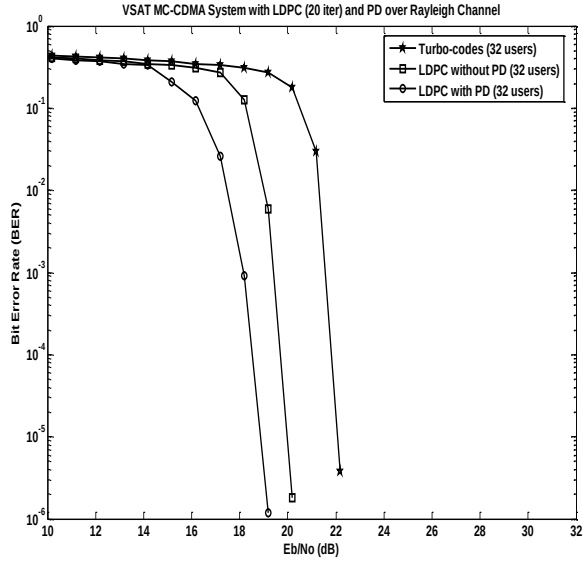

Fig.16 Performance of VSAT MC-CDMA system using LDPC codes and predistortion technique (For 32 users)

In Figure 16, we can observe that for a BER=10^{-5} the system using LDPC coding provides an additional gain of 2 dB compared to the system coded by turbo codes. We can notice also that, after the integration of LDPC coding in communication chain, system performance reaches a lower value of BER compared to that reached by the adoption of Turbo coding.

In the figure above, we observe that the adoption of the predistortion technique improves the system performance in terms of bit error rate. Indeed, for a BER of 10^{-5}, the system adopting the LDPC codes in conjunction with the predistortion technique provides a gain of about 1 dB compared to the system using the LDPC codes without predistortion process.

In figure 17 we presented the performance of the communication system using LDPC codes for a variation of the size of the code blocks.

In general, we note that the performance gradually improved when the block code size increases. For large blocks of code, LDPC coding can result very close to the Shannon limit performance. But, we find that increasing the code block size leads to increased complexity of the decoding system.

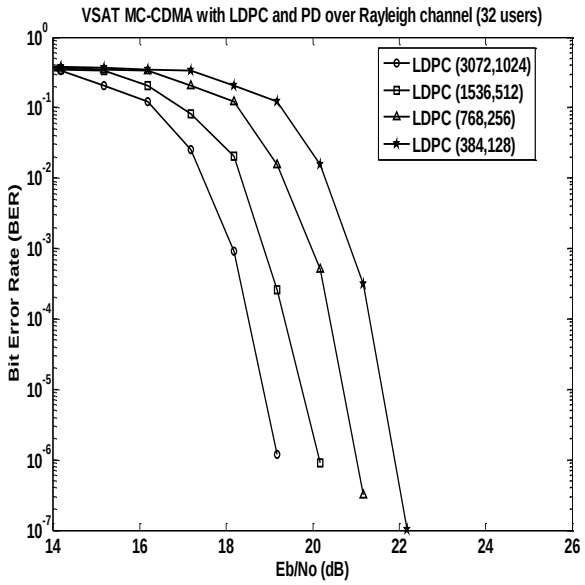

Fig.17 impact of the block length on performance of VSAT MC-CDMA system (For 32 users)

9 Conclusion

In this paper, the performance in uplink of VSAT MC-CDMA system has been investigated by using the Ku band and the most popular type of multiple access technique, Code Division Multiple Access

(CDMA) combining with multicarrier transmission system. To get the lower bit error rate, the most common types of channel coding methods (LDPC codes, Turbo codes and convolutional codes) are used. To compensate the effect of the non-linearity in the system, a predistortion technique adapted to the SSPA amplifier was adopted. The results show that the performance depends upon the number of active users in the network and performance of encoding/decoding mechanisms.

In conclusion, for a similar code rate we can see that despite the performance offered by the coding structures "Turbo and Convolutional" these coding strategies are less reliable and efficient process compared to LDPC coding. Because this mechanism presented a great potential for improvement and optimization. we can add that the increasing of the code length improves performance but also increases the complexity of the decoding system. it was noted that the integration of the predistortion technique further improves the performance of the coded system.

References:

[1] Maral, G. 1996. VSAT Networks. New York: John Wiley & Sons Ltd.

[2] Evans, B.G., Satellite Communication Systems, 3rd ed., United Kingdom. The Institution of Electrical Engineers, 1999.

[3] Elbert, B.R., The Satellite Communication Ground Segment and Earth Station Handbook, Artech House, 2000.

[4] Elbert, B.R., Introduction to Satellite Communication 3rd , Artech House, 2008.

[5] Moheb, H., C. Robinson, J. Kijeski, "Design and Development of Co-Polarized Ku-band Ground Terminal System for VSAT Application," IEEE Publications 0-7803-5639-X/99, pp. 2158-2161, 1999.

[6] H. E. Ghazi, "Allocation Algorithm for Optimizing MC-CDMA Over Correlated Channel"accepted by WSEAS Trans. On commun.2010.

[7] Q. Shi and M. Latva-Aho, "Performance analysis of MC-CDMA in Rayleigh fading channels with correlated envelopes and phases," IEE Proc. Commun., vol. 150, pp. 214–220, June 2003.

[8] M. El jourmi, "Performance analysis of channel coding in satellite communicationbased on VSAT Network and MC-CDMA scheme" WSEAS Trans. on commun., issue 5, vol 12, May 2013.

[9] Q. Shi and M. Latva-Aho, "Performance analysis of MC-CDMA in Rayleigh fading channels with correlated envelopes and phases," IEE Proc. Commun., vol. 150, pp. 214–220, June 2003.

[10] 3GPP, \3GPP TS 45.003 V7.5.0." Internet, 2008.

[11] Peter Clements, Paul Nettle, and Ryan Gallagher. Parity volume set specification 2.0, May 11th 2003.

[12] A. N. D'Andrea, V. Lottici and R. Reggiannin, «Nonlinear Predistortion of OFDM Signals over Frequency-Selective Fading Channels», IEEE Transactions on Communications. Vol. 49. N° 5. pp. 837-843. 2001.

[13] R. zayani, S. Zid, R. Bouallegue, « Simulateur des non-linéarités HPA sur un système OFDM » OHD Conference, septembre 2005.

[14] P.B. Kenington, "High-linearity RF amplifier design", Artech house, pp.351-423, 2000.